

中村隆広、住友直方	EBMに基づく小児不整脈治療	五十嵐隆	薬物療法とカテーテル治療、EBM小児疾患の治療2011-2012	中外医学社	東京	2011	112-119
阿部百合子、住友直方	小児の不整脈について	奥村 謙	ガイドライン/ガイドランス 不整脈	日本医事新報社	東京	2011	87-93
阿部百合子、住友直方	カテコラミン誘発性多形性心室頻拍	池田隆徳	ステップアップのための不整脈診療ガイドブック	MEDICAL VIEW社	東京	2011	328-334
松村昌治、住友直方	小児の不整脈	山下武志	あなたも名医！ ああ～どうする？！この不整脈	日本医事新報社	東京	2011	118-123
長嶋正實、住友直方、牛ノ濱大也、前野泰樹		長嶋正實、住友直方、牛ノ濱大也、前野泰樹	小児不整脈、改訂第2版	診断と治療社	東京	2011	pp10-17, pp36-37, pp55-73, pp88-103, pp106-107, 111-116, pp117-143, pp144-150、
阿部百合子、住友直方	カテコラミン誘発性多形性心室頻拍と遺伝子異常	井上 博	Medical Topics Series不整脈2011	MEDICAL VIEW社	東京	2011	148-157
金丸 浩、住友直方	就学・学校生活での注意事項	奥村 謙	ペースメーカー・ICD・CRT/CRT-Dトラブルシューティングからメンタルケアまで	MEDICAL VIEW社	東京	2011	222-227
住友直方	WPW症候群	大関武彦、古川 漸、横田俊一郎、水口雅	今日の小児治療指針第15版	医学書院	東京	2011	502-503

雑誌

発表者氏名	論文タイトル名	発表誌名	巻号	ページ	出版年
Shimada T, Ohku bo K, Watanabe I, <u>Makita N.</u>	A novel 5' splice site mutation of SCN5A associated with Brugada syndrome resulting in multiple cryptic transcripts.	Int J Cardiol		in press	2012
<u>Watanabe H, Makita N, Tanabe N, Watanabe T, Aizawa Y.</u>	Electrocardiographic abnormalities and risk of complete atrioventricular block.	Int J Cardiol	155	462-464	2012
Delmar M, <u>Makita N.</u>	Cardiac Connexins, Mutations and Arrhythmias.	Curr Opin Cardiol		236-241	2012

<p><u>Watanabe H</u>, Nogami A, Ohkubo K, Kawata H, Hayashi Y, Ishikawa T, <u>Makiyama T</u>, Nagao S, Yagi hara N, Takehara N, Kawamura Y, Sato A, Okamura K, Hosaka Y, Sato M, Fukae S, Chinushi M, Oda H, Okabe M, Kimura A, Maemura K, Watanabe I, Kamakura S, <u>Horie M</u>, Aizawa Y, <u>Shimizu W</u>, <u>Makita N</u>.</p>	<p>Response to Letter Regarding Article, "Electrocardiographic Characteristics and SCN5A Mutations in Idiopathic Ventricular Fibrillation Associated With Early Repolarization".</p>	<p>Circ: Arrhythm Electrophys</p>	<p>e60-e61</p>	<p>2012</p>
<p><u>Makita N</u>.</p>	<p>Phenotypic overlap of lethal arrhythmias associated with cardiac sodium mutations. Individual-specific or mutation-specific?</p>	<p>Genes and Cardiovascular Function</p>	<p>185-196</p>	<p>2012</p>
<p><u>Makita N</u>, <u>Seki A</u>, <u>Sumitomo N</u>, Chkourko H, Fukuhara S, <u>Watanabe H</u>, <u>Shimizu W</u>, Bezzina CR, Hasdemir C, Mugishima H, <u>Makiyama T</u>, Baruteau A, Baron E, <u>Horie M</u>, Hagiwara N, Wilde AA, Probst V, Le Marec H, Roden DM, Mochizuki N, Schott JJ, Delmar M.</p>	<p>A connexin40 mutation associated with a malignant variant of progressive familial heart block type I.</p>	<p>Circ Arrhythm Electrophysiol</p>	<p>163-172</p>	<p>2012</p>
<p>Aizawa Y, Sato A, Watanabe H, Chinushi M, Furushima H, <u>Horie M</u>, Kaneko Y, Imaizumi T, Okubo K, Watanabe I, Shinozaki T, Aizawa Y, Fukuda, Joo K, Haissaguerre M.</p>	<p>Dynamicity of the J wave in idiopathic ventricular fibrillation with a special reference to pause-dependent augmentation of the J wave.</p>	<p>Journal of American College of Cardiology</p>	<p>in press</p>	
<p>Kuramoto Y, Furukawa Y, Yamada T, Okuyama Y, <u>Horie M</u>, Fukunami M.</p>	<p>Andersen-Tawil Syndrome Associated With Aborted Sudden Cardiac Death: Atrial Pacing Was Effective for Ventricular Arrhythmias.</p>	<p>AJMS</p>	<p>in press</p>	
<p>Okayasu H, Ozeki Y, Fujii K, Takano Y, Saeki Y, Hori H, <u>Horie M</u>, Higuchi T, Kunugi H, Shimoda K.</p>	<p>Pharmacotherapeutic determinants for QTc interval prolongation in Japanese patients with mood disorder.</p>	<p>Pharmacopsychiatry</p>	<p>in press</p>	

Hattori T, <u>Makiyama T</u> , Akao M, Ehara E, Ohno S, Iguchi M, Nishio Y, Sasaki K, Itoh H, Yokode M, Kita T, <u>Horie M</u> , Kimura T.	A novel gain-of-function KCNJ2 mutation associated with short QT syndrome impairs inward rectification of Kir2.1 currents.	Cardiovascular Research	934	666-673	2012
Wu J, Ding WG, Matsuura H, <u>Horie M</u> .	Regulatory mechanisms underlying the modulation of GIRK1/GIRK4 heteromeric channels by P2Y receptors.	Pflugers Archiv	463(4)	625-633	2012
Yamazaki M, Honjo H, Ashihara T, Harada M, Sakuma I, Nakazawa K, Trayanova N, <u>Horie M</u> , Kalifa J, Jalife J, Kamiya K, Kodama I.	Regional cooling facilitates termination of spiral-wave reentry through unpinning of rotors in rabbit hearts.	Heart Rhythm	9	107-114	2012
Kaneshiro T, Naruse Y, Nogami A, Tada H, Yoshida K, Sekiguchi Y, Murakoshi N, Kato Y, Horigome H, Kawamura M, <u>Horie M</u> , Aonuma K.	Successful catheter ablation of bidirectional ventricular premature contractions triggering ventricular fibrillation in catecholaminergic polymorphic ventricular tachycardia with RyR2 mutation.	Circulation Arrhythmia and Electrophysiology	5	e14-e17	2012
Miyamoto A, Hayashi H, Yoshino T, Kawaguchi T, Taniguchi A, Ito H, Sugimoto Y, Ito M, <u>Makiyama T</u> , Xue JQ, Murakami Y, <u>Horie M</u> .	Clinical and electrocardiographic characteristics of patients with short QT interval in a large hospital-based population.	Heart Rhythm	9(1)	66-74	2012
Costa J, Lopes CM, Barsheshet A, Moss AJ, Migdalovich D, Ouellet G, McNitt S, Polonsky S, Robinson JL, Zareba W, Ackerman MJ, Benhorin J, Kaufman ES, Platonov PG, <u>Shimizu W</u> , Towbin JA, Vin-cent GM, Wilde AA, Golden-berg I	Combined assessment of sex- and mutation-specific information for risk stratification in type 1 long QT syndrome	Heart Rhythm	9	in press	2012
Baranchuk A, Nguyen T, Ryu MH, Femenía F, Zareba W, Wilde AAM, <u>Shimizu W</u> , Brugada P, Pérez-Riera AR	Brugada phenocopy: new terminology and proposed classification.	Ann Noninvasive Electro-cardiol		in press	2012

Nakashima K, Kusakawa I, Yamamoto T, Hirabayashi S, Hosoya R, <u>Shimizu W</u> , <u>Sumitomo N</u> .	A left ventricular noncompaction in a patient with long QT syndrome caused by a KCNQ1 mutation: a case report.	Heart Vessels		in press	2012
Barsheshet A, Goldenberg I, O-Uchi J, Moss AJ, Christian Jons C, <u>Shimizu W</u> , Wilde AA, McNitt S, Peterson DR, Zareba W, Robinson JL, Ackerman MJ, Cypress M, Gray DA, Hofman N, Kanters JK, Kaufman ES, Platonov PG, Qi M, Towbin JA, Vincent GM, Lopes CM	Mutations in cytoplasmic loops of the KCNQ1 channel and the risk of life-threatening events. Implications for mutation-specific response to beta-blocker therapy in type-1 long QT syndrome.	Circulation	125	1988-96	2012
Hoefen R, Reumann M, Goldenberg I, Moss AJ, O-Uchi j, Gu Y, McNitt S, Zareba W, Jons C, Kanters JK, Platonov PG, <u>Shimizu W</u> , Wilde AAM, Rice JJ, Lopes CM	In silico cardiac risk assessment of Long QT patients:clinical predictability of cardiac models.	J Am Coll Cardiol		in press	2012
Kawata H, Noda T, Yamada Y, Okamura H, Satomi K, Aiba T, Takaki H, Aihara N, Isobe M, Kamakura S, <u>Shimizu W</u> .	Effect of sodium-channel blockade on early repolarization in inferior/lateral leads in patients with idiopathic ven-tricular fibrillation and Brugada syn-drome.	Heart Rhythm	9	77-83	2012
Makimoto H, Kamakura S, Aihara N, Noda T, Nakajima I, Yokoyama T, Doi A, Kawata H, Yamada Y, Okamura H, Satomi K, Aiba T, <u>Shimizu W</u> .	Clinical impact of the number of extrastimuli in programmed electrical stimulation in patients with Brugada type 1 electrocardiogram.	Heart Rhythm	9	242-248	2012
Noto N, Okada T, Abe Y, Miyashita M, Kanamaru H, Karasawa K, Ayusawa M, <u>Sumitomo N</u> , Mugishima H.	Characteristics of earlier atherosclerotic involvement in adolescent patients with Kawasaki disease and coronary artery lesions: Significance of gray scale median on B-mode ultrasound	Atherosclerosis	221	106-9	2012

Miyoshi T, Maeno Y, Sago H, Inamura N, Yasukohchi S, Ka-wataki M, Horigome H, Yoda H, Taketazu M, Shozu M, Nii M, Kato H, Hayashi S, Hagiwara A, Omoto A, <u>Shimizu W</u> , Shiraishi I, Sakaguchi H, Nishimura K, Ueda K, Katsuragi S, Ikeda T.	Evaluation of transplacental treatment for fetal congenital bradyarrhythmia: A nationwide survey in Japan.	Circ J	76	469-476	2012
Kobayashi T, Saji T, Otani T, Takeuchi K, Nakamura T, Arakawa H, Kato T, Hara T, Hamaoka K, Ogawa S, Miura M, Nomura Y, Fuse S, Ichida F, Seki M, Fukazawa R, Ogawa C, Furuno K, Tokunaga H, Takatsuki S, Hara S, Morikawa A, on behalf of the RAISE study group investigators	Efficacy of immunoglobulin plus prednisolone for prevention of coronary artery abnormalities in severe Kawasaki disease (RAISE study): a randomised, open-label, blinded-endpoints trial	Lancet	28	1613-1620	2012
Kato Y, Horigome H, Takahashi-Igari M, <u>Sumitomo N</u> , Aonuma K.	Tachycardia associated with twin atrioventricular nodes in an infant with heterotaxy and interruption of inferior vena cava	Pacing and Clinical Electrophysiology	32	in press	2012
Takahashi I, Abbot RD, Ohshita T, Takahashi T, Ozasa K, <u>Akahoshi M</u> , Fujiwara S, Kodama K, Matsumoto M.	A prospective follow-up study of the association of radiation exposure with fatal and non-fatal stroke among atomic bomb survivors in Hiroshima and Nagasaki (1980-2003).	BMJ Open.	2	e000654	2012
Adams MJ, Grant EJ, Kodama K, Shimizu Y, Kasagi F, Suyama A, Sakata R, <u>Akahoshi M</u> .	Radiation dose associated with renal failure mortality: a potential pathway to partially explain increased cardiovascular disease mortality observed after whole-body irradiation.	Radiat Res.	177	220-8	2012
Hida A, <u>Akahoshi M</u> , Takagi Y, Imaizumi M, Sera N, Soda M, Maeda R, Nakashima E, Ida H, Kawakami A, Nakamura T, Eguchi K.	Lipid infiltration in the parotid glands: a clinical manifestation of metabolic syndrome.	Exp Clin Endocrinol Diabetes.	120	110-5	2012

Imaizumi M, Sera N, Ueki I, Horie I, Ando T, Usa T, Ichimaru S, Nakashima E, Hida A, Soda M, Tominaga T, Ashizawa K, Maeda R, Nagataki S, <u>Akahoshi M.</u>	Risk for progression to overt hypothyroidism in an elderly Japanese population with subclinical hypothyroidism.	Thyroid.	21	1177-82	2012
<u>Watanabe H.</u> , Tanabe N, Yagihara N, Watanabe T, Aizawa Y, Kodama M.	Cholesterol paradox in atrial fibrillation	Circ J		in press	2012
Furushima H, Chinushi M, Iijima K, Hasegawa K, Sato A, Izumi D, <u>Watanabe H.</u> , Aizawa Y.	Is the coexistence of sustained ST segment elevation and abnormal q waves a risk factor for electrical storm in implanted cardioverter defibrillator patients with structural heart diseases?	Europace	14	675-681	2012
Yagihara N, Sato A, Iijima K, Izumi D, Furushima H, <u>Watanabe H.</u> , Irie T, Kaneko Y, Kurabayashi M, Chinushi M, Sato U M, Aizawa Y.	The prevalence of early repolarization in wolff-parkinson-white syndrome with a special reference to j waves and the effects of catheter ablation.	J Electrocardiol	45	36-42	2012
Sato A, Tanabe Y, Chinushi M, Hayashi Y, Yoshida T, Ito E, Izumi D, Iijima K, Yagihara N, <u>Watanabe H.</u> , Furushima H, Aizawa Y.	Analysis of J waves during myocardial ischaemia.	Europace	14	715-23	2012
<u>蒔田直昌</u>	特発性心室細動とJ波症候群の遺伝子診断	CIRCULATION Up-to-Date	7	20-25	2012
長野伸彦、鮎沢衛、阿部百合子、長谷川真紀、田口洋祐、中村隆広、福原淳示、市川理恵、松村昌治、宮下理夫、金丸浩、 <u>住友直方</u> 、岡田知雄、麦島秀雄	肺炎球菌感染により致死経過をたどった無脾症候群の2例	日本小児科学会雑誌	116	537-541	2012

Watanabe H, Nogami A, Ohkubo K, Kawata H, Hayashi Y, Ishikawa T, Nagao S, Yagihara N, Takehara N, Kawamura Y, Sato A, Okamura K, Hosaka Y, Sato N, Fukae S, Chinushi M, Oda H, Okabe M, Kimura A, Maemura K, Watanabe I, Kamakura S, Aizawa Y, <u>Shimizu W</u> , <u>Makita N</u>	Electrocardiographic Characteristics and SCN5A Mutations in Idiopathic Ventricular Fibrillation Associated with Early Repolarization.	Circ Arrhythm Electrophysiol	4	874-881	2011
Li P, Ninomiya H, Kurata Y, Kato M, Miake J, Yamamoto Y, Igawa O, Nakai A, Higaki K, Toyoda F, Wu J, <u>Horie M</u> , Shirayoshi Y, Hiraoka M, Hisatome I.	Reciprocal control of hERG stability by Hsp70 and Hsc70 with implication for restoration of LQT2 mutant stability.	Circulation Research	108	458-468	2011
Miyamoto A, Hayashi H, <u>Makiyama T</u> , Yoshino T, Mizusawa Y, Sugimoto Y, Ito M, Xue JQ, Murakami Y, <u>Horie M</u> .	Risk determinants in individuals with a spontaneous type 1 Brugada ECG.	Circulation Journal	75	844-851	2011
Ohno S, Zankov DP, Ding WG, Itoh H, <u>Makiyama T</u> , Doi T, Shizuta S, Hattori T, Miyamoto A, Naiki N, Hancox JC, Matsuura H, <u>Horie M</u> .	KCNE5 (KCNE1L) variants are novel modulators of brugada syndrome and idiopathic ventricular fibrillation.	Circulation: Arrhythmia and Electrophysiology	4(3)	352-361	2011
Doi T, <u>Makiyama T</u> , Morimoto T, Haruna Y, Tsuji K, Ohno S, Akao M, Takahashi Y, Kimura T, <u>Horie M</u> .	A novel KCNJ2 nonsense mutation, S369X, impedes trafficking and causes a limited form of andersen-tawil syndrome.	Circulation: Cardiovascular Genetics	4	253-260	2011
<u>Shimizu W</u> , <u>Horie M</u> .	Phenotypical manifestations of mutations in genes encoding subunits of cardiac potassium channels.	Circulation Research	109	97-109	2011
Tsuji -Wakisaka K, Akao M, Ishii TM, Ashihara T, <u>Makiyama T</u> , Ohno S, Toyoda F, Nishio Y, Sakaguchi T, Matsuura H, <u>Horie M</u> .	Identification and functional characterization of KCNQ1 mutations around the exon7-intron7 junction affecting the splicing process.	Biochem Biophys Acta-Molecular Basis of Disease	1812	1524- 1559	2011

Hayashi H, <u>Horie M.</u>	Heritability of early repolarization: A population-based study.	Circulation Cardiovascular Genetics	4	e20	2011
Kimura H, Mizusawa Y, Itoh H, Miyamoto A, Kawamura M, Kawaguchi T, Naiki N, Oka Y, Ohno S, <u>Makiyama T</u> , Ito M, <u>Horie M.</u>	Carvedilol, a non-selective $\beta$ -with $\alpha$ 1-blocker is effective in long QT syndrome type2.	Journal of Arrhythmia	27	324-331	2011
Miyamoto A, Hayashi H, Ito M, <u>Horie M.</u>	Remission of abnormal conduction and repolarization in the right ventricle after chemotherapy in patients with anterior mediastinal tumor.	J Cardiovasc Electrophysiol.	22	350	2011
Aiba T, <u>Shimizu W.</u>	Editorial Commentary. Molecular screening of long-QT syndrome: risk is there or rare?	Heart Rhythm	8	420-421	2011
Goldenberg I, Horr S, Moss AJ, Lopes CM, Barshesh et A, McNitt S, Zareba W, Andrews ML, Robinson JL, Locati EH, Ackerman MJ, Benhorin J, Kaufman ES, Napolitano C, Platonov PG, Priori SG, Qi M, Schwartz PJ, <u>Shimizu W</u> , Towbin JA, Vincent GM, Wilde AA, Zhang L.	Risk for Life-threatening cardiac events in patients with genotype-confirmed long-QT syndrome and normal-range corrected QT inter-vals.	J Am Coll Cardiol	57	51-59	2011
Jons C, O-Uchi J, Moss AJ, Reumann M, Rice JJ, Goldenberg I, Zareba W, Wilde AA, <u>Shimizu W</u> , Kanters JK, McNitt S, Hofman N, Robinson JL, Lopes CM.	Use of mutant-specific ion channel characteristics for risk stratification of long QT syndrome patients.	Sci Transl Med	3	76ra28	2011
Migdalovich D, Moss AJ, Lopes CM, Costa J, Ouellet G, Barshesht A, McNitt S, Polonsky S, Robinson JL, Zareba W, Ackerman MJ, Benhorin J, Kaufman ES, Platonov PG, <u>Shimizu W</u> , Towbin JA, Vincent GM, Wilde AA, Goldenberg I	Mutation and gender specific risk in type-2 long QT syndrome: Implications for risk stratification for life-threatening cardiac events in patients with long QT syndrome.	Heart Rhythm	8	1537-1543	2011



van der Werf C, Kannankeril PJ, Sacher F, Krahn AD, Viskin S, Leenhardt S, <u>Shimizu W</u> , <u>Sumitomo N</u> , Fish FA, Bhuiyan ZA, Willems AR, van der Veen MJ, <u>Watanabe H</u> , Laborderie J, Haissaguerre M, Knollmann BC, Wilde AAM	Flecainide therapy reduces exercise-induced ventricular arrhythmias in patients with catecholaminergic polymorphic ventricular tachycardia.	J Am Coll Cardiol	57	2244-2254	2011
Chinen S, Miura M, Tamame T, Matsuoka M, Ohki H, <u>Sumitomo N</u> .	Life-threatening Atrial Tachycardia after the Senning Operation in a Patient with Transposition of the Great Arteries	Heart and Vessels	20	in press	2011
Fukuhara J, <u>Sumitomo N</u> , Nakamura N, Ichikawa R, Matsumura M, Abe O, Miyashita M, Kanamaru H, Ayusawa M, Karasawa K, Mugishima H.	Electrophysiological characteristics of idiopathic ventricular tachycardia in children.	Circ J	75	672-6	2011
Ichikawa R, <u>Sumitomo N</u> , Komori A, Abe Y, Nakamura T, Fukuhara J, Matsumura M, Miyashita M, Kanamaru H, Ayusawa M, Mugishima H.	The follow-up evaluation of electrocardiograms and arrhythmias in children with fulminant myocarditis.	Circ J	75	932-8	2011
Noto N, Okada T, Abe Y, Miyashita M, Kanamaru H, Karasawa K, Ayusawa M, <u>Sumitomo N</u> , Mugishima H.	Changes in the Textural Characteristics of Intima-Media Complex in Young Patients with Familial Hypercholesterolemia: Implication for Visual Inspection on B-Mode Ultrasound	Journal of American Society of Echocardiography	24	438-43	2011
Horigome H, Ishikawa Y, Shiono J, Iwamoto M, <u>Sumitomo N</u> , Yoshinaga M.	Detection of extra-components of T wave by independent component analysis in congenital long QT syndrome.	Circ Arrhythm Electrophysiol	4	456-64	2011
<u>Sumitomo N</u> .	Are there Juvenile and Adult types in patients with Catecholaminergic Polymorphic Ventricular Tachycardia	Heart and Vessels	8	872-3	2011

Yoshida K, Ohishi W, Nakashima E, Fujiwara S, Akahoshi M, Kasagi F, Chayama K, Hakoda M, Kyoizumi S, Nakachi K, Hayashi T, Kusunoki Y.	Lymphocyte subset characterization associated with persistent hepatitis C virus infection and subsequent progression of liver fibrosis.	Hum Immunol.	72	821-6	2011
Haruta D, Matsuo K, Tsuneto A, Ichimaru S, Hida A, Sera N, Imaizumi M, Nakashima E, Maemura K, Akahoshi M.	Incidence and prognostic value of early repolarization pattern in the 12-lead electrocardiogram.	Circulation.	123	2931-7	2011
Fukushima N, Matsura K, Akazawa H, Honda A, Nagai T, Takahashi M, Seki A, Murasaki K, Shimizu T, Okano M, Hagiwara N, Komuro I.	A crucial role of activin A-mediated growth hormone suppression in mouse and human heart failure.	PLoS One.	6(12)	e27901	2011
Watanabe H, Yang T, Stroud DM, Lowe JS, Harris L, Atack TC, Wang DW, Hipkens SB, Leake B, Hall L, Kupersmidt S, Chopra N, Magnuson MA, Tanabe N, Knollmann BC, George AL, Jr., Roden DM.	Striking in vivo phenotype of a disease-associated human scn5a mutation producing minimal changes in vitro.	Circulation	124	1001-1011	2011
Watanabe H, Tanabe N, Yagihara N, Watanabe T, Aizawa Y, Kodama M.	Association between lipid profile and risk of atrial fibrillation.	Circ J	75	2767-2774	2011
Watanabe H, Steele DS, Knollmann BC.	Mechanism of antiarrhythmic effects of flecainide in catecholaminergic polymorphic ventricular tachycardia.	Circ Res	109	712-713	2011
Watanabe H, Knollmann BC.	Mechanism underlying catecholaminergic polymorphic ventricular tachycardia and approaches to therapy.	J Electrocardiol	44	650-655	2011
Sato A, Chinushi M, Iijima K, Watanabe H, Izumi D, Furushima H, Sonoda K, Hasegawa K, Yagihara N, Aizawa Y.	An appropriate defibrillation threshold obtained by the combined connection between two shock leads and icd generator.	Intern Med	50	2815-2818	2011

Oda M, <u>Watanabe H</u> , Oda E, Tomita M, Obata H, Ozawa T, Oda Y, Iizuka T, Toba K, Aizawa Y.	Rise in international normalized ratio after a catastrophic earthquake in patients treated with warfarin.	Int J Cardiol	152	109-110	2011
Nagao S, Hayashi Y, Yagihara N, Sato A, <u>Watanabe H</u> , Furushima H, Chinushi M, Aizawa Y.	Preexcitation unmasks j waves: 2 cases.	Electrocardiol	44	359-362	2011
Atack TC, Myers Stroud D, <u>Watanabe H</u> , Yang T, Hall L, Hipkens SB, Lowe JS, Leake B, Magnuson MA, Yang P, Roden DM.	Informatic and functional approaches to identifying a regulatory region for the cardiac sodium channel.	Circ Res	109	38-46	2011
Chinushi M, Iijima K, Furushima H, Izumi D, Sato A, Yagihara N, Hasegawa K, <u>Watanabe H</u> , Soejima K, Aizawa Y.	Suppression of Storms of Ventricular Tachycardia by Epicardial Ablation of Isolated Delayed Potential in Noncompaction Cardiomyopathy.	Pacing Clin Electrophysiol		1-5	2011
<u>蒔田直昌</u>	不整脈とイオンチャンネル病	別冊・医学のあゆみ		5-12	2011
<u>蒔田直昌</u>	遺伝性心臓伝導障害の分子基盤	循環器内科	70	460-467	2011
<u>蒔田直昌</u>	致死性不整脈の基礎と臨床－特発性心室細動－	臨床と研究	88	127-129	2011
<u>蒔田直昌</u>	後天性QT延長症候群の新しい展開	不整脈+PLUS		3-8	2011
佐野 幹、渡邊栄一、 <u>牧山 武</u> 、内山達司、祖父江嘉洋、奥田健太郎、山本真由美、 <u>堀江 稔</u> 、尾崎行男	ペースメーカー植え込み同胞霊位認められた新たなLamin A/C変異	心電図	31	18-24	2011
伊藤英樹、 <u>堀江 稔</u> 、井本敬二	遺伝性不整脈疾患とシミュレーション。	不整脈+PLUS	3	9	2011
定 翼、国分則人、 <u>堀江 稔</u> 、阿部百佳、駒ヶ嶺朋	KCNJ2変異を伴う Andersen-Tawil症候群の神経生理所見。	臨床神経生理学	39	18-23	2011
<u>堀江 稔</u>	循環器疾患における遺伝的背景と発症機序理解のための多面的アプローチ	循環器内科	70	421-422	2011
脇坂啓子、 <u>堀江 稔</u>	スプライシング異常と循環器疾患	循環器内科	70	523-529	2011

中村隆広、住友直方、阿部百合子、市川理恵、福原淳示、松村昌治、金丸 浩、鮎沢衛、岡田知雄、麦島秀雄、中井俊子、平山篤志	難治性心室頻拍を伴った拡張型心筋症の1例	心臓	43(supple 3)	177-183	2011
牧山 武	循環器疾患の発症機序解明におけるiPS細胞の可能性	循環器内科	70	530-536	2011

#### IV. 研究成果の刊行物・別刷り

# A Connexin40 Mutation Associated With a Malignant Variant of Progressive Familial Heart Block Type I

Naomasa Makita, MD, PhD; Akiko Seki, MD, PhD; Naokata Sumitomo, MD, PhD;  
Halina Chkourko, MS; Shigetomo Fukuhara, PhD; Hiroshi Watanabe, MD, PhD;  
Wataru Shimizu, MD, PhD; Connie R. Bezzina, PhD; Can Hasdemir, MD; Hideo Mugishima, MD;  
Takeru Makiyama, MD, PhD; Alban Baruteau, MD; Estelle Baron, BS; Minoru Horie, MD, PhD;  
Nobuhisa Hagiwara, MD, PhD; Arthur A.M. Wilde, MD; Vincent Probst, MD, PhD;  
Hervé Le Marec, MD; Dan M. Roden, MD; Naoki Mochizuki, MD, PhD;  
Jean-Jacques Schott, PhD; Mario Delmar, MD, PhD

**Background**—Progressive familial heart block type I (PFHBI) is a hereditary arrhythmia characterized by progressive conduction disturbances in the His-Purkinje system. PFHBI has been linked to genes such as *SCN5A* that influence cardiac excitability but not to genes that influence cell-to-cell communication. Our goal was to explore whether nucleotide substitutions in genes coding for connexin proteins would associate with clinical cases of PFHBI and if so, to establish a genotype-cell phenotype correlation for that mutation.

**Methods and Results**—We screened 156 probands with PFHBI. In addition to 12 sodium channel mutations, we found a germ line *GJA5* (connexin40 [Cx40]) mutation (Q58L) in 1 family. Heterologous expression of Cx40-Q58L in connexin-deficient neuroblastoma cells resulted in marked reduction of junctional conductance (Cx40-wild type [WT],  $22.2 \pm 1.7$  nS, n=14; Cx40-Q58L,  $0.56 \pm 0.34$  nS, n=14;  $P < 0.001$ ) and diffuse localization of immunoreactive proteins in the vicinity of the plasma membrane without formation of gap junctions. Heteromeric cotransfection of Cx40-WT and Cx40-Q58L resulted in homogenous distribution of proteins in the plasma membrane rather than in membrane plaques in  $\approx 50\%$  of cells; well-defined gap junctions were observed in other cells. Junctional conductance values correlated with the distribution of gap junction plaques.

**Conclusions**—Mutation Cx40-Q58L impairs gap junction formation at cell-cell interfaces. This is the first demonstration of a germ line mutation in a connexin gene that associates with inherited ventricular arrhythmias and emphasizes the importance of Cx40 in normal propagation in the specialized conduction system. (*Circ Arrhythm Electrophysiol.* 2012; 5:163-172.)

**Key Words:** heart block ■ genes ■ ion channels ■ death sudden ■ gap junctions

Cardiac myocyte excitability in atria, His-Purkinje system, and ventricles is largely determined by the properties of voltage-gated sodium channels. Once activated, excitatory currents rapidly propagate to neighboring cells through low-resistance intercellular channels called gap junctions, which facilitate the synchronous contraction of the heart.<sup>1,2</sup> Loss of expression and function of cardiac gap junctions and sodium currents can severely impair action potential propagation,

which sets the stage for life-threatening arrhythmias.<sup>1,2</sup> Although multiple mutations in genes coding for components of the voltage-gated sodium channel complex have been previ-

## Clinical Perspective on p 172

ously described in relation to arrhythmias and sudden death in young persons<sup>3</sup> and connexin40 (Cx40) mutations have been implicated in atrial fibrillation,<sup>4,5</sup> no study has identified an

Received September 24, 2011; accepted January 9, 2012.

From the Department of Molecular Pathophysiology, Graduate School of Biomedical Sciences, Nagasaki University, Nagasaki, Japan (N. Makita); Cardiology, Tokyo Women's Medical University, Tokyo, Japan (A.S., N.H.); Pediatrics and Child Health, Nihon University School of Medicine, Tokyo, Japan (N.S., H.M.); Cardiology, New York University Medical School, New York, NY (H.C., M.D.); Cell Biology, National Cerebral and Cardiovascular Center Research Institute, Suita, Japan (S.F., N. Mochizuki); Cardiology, Niigata University Graduate School of Medical and Dental Sciences, Niigata, Japan (H.W.); Cardiology, National Cerebral and Cardiovascular Center, Suita, Japan (W.S.); Experimental Cardiology, Academic Medical Center, University of Amsterdam, Amsterdam, The Netherlands (C.R.B., A.A.M.W.); Cardiology, Ege University School of Medicine, Bornova, Izmir, Turkey (C.H.); Cardiovascular Medicine, Kyoto University Graduate School of Medicine, Kyoto, Japan (T.M.); l'institut du thorax, INSERM UMR915, Nantes, France (E.B., V.P., H.L., J.-J.S.); Cardiovascular Medicine, Shiga University of Medical Science, Otsu, Japan (M.H.); and Pharmacology and Medicine, Vanderbilt University, Nashville, TN (D.M.R.).

The online-only Data Supplement is available with this article at <http://circep.ahajournals.org/lookup/suppl/doi:10.1161/CIRCEP.111.967604/-/DC1>.

Correspondence to Naomasa Makita, MD, PhD, Department of Molecular Pathophysiology, Graduate School of Biomedical Sciences, Nagasaki University, 1-12-4 Sakamoto, 852-8523 Nagasaki, Japan. E-mail makitan@nagasaki-u.ac.jp

© 2012 American Heart Association, Inc.

*Circ Arrhythm Electrophysiol* is available at <http://circep.ahajournals.org>

DOI: 10.1161/CIRCEP.111.967604

association between germ line mutations in gap junction proteins and inherited ventricular arrhythmias in humans.

In this study, we investigated a group of patients with progressive familial heart block type I (PFHBI) (Online Mendelian Inheritance in Man 113900), also known as progressive cardiac conduction defect or Lenègre-Lev disease,<sup>6,7</sup> is a dominant inherited disorder of the His-Purkinje system. Affected individuals show electrocardiographic evidence of bundle branch disease (ie, right bundle branch block, left anterior or posterior hemiblock, complete heart block) with broad QRS complexes. The disease can progress from a normal ECG to right bundle branch block and from the latter to complete heart block. Affected individuals often present with family history of syncope, pacemaker implantation, and sudden death.<sup>8</sup> Although structural abnormalities have been invoked as a cause of the disease,<sup>6,7</sup> a number of patients present with normal cardiac structure and contractile function. Linkage analysis in a large South African PFHBI kindred<sup>9</sup> and a Lebanese kindred<sup>10</sup> mapped a causal locus on chromosome 19q13.3, and further work identified mutations in genes encoding for the transient receptor potential nonselective cation channel, subfamily M, member 4 (*TRPM4*) gene<sup>11</sup> at this locus. Haploinsufficiency of *SCN5A* and aging have been implicated in PFHBI,<sup>8</sup> and age-dependent manifestations of the disease have been recapitulated in mice.<sup>12</sup>

Here, we sought to expand on the association between PFHBI and mutations in genes relevant to action potential propagation; in particular, we assessed the possible association between nucleotide substitutions in connexin-coding genes and PFHBI. We evaluated 156 probands of diverse ethnic backgrounds from Asia, Europe, and North America given a clinical diagnosis of PFHBI. In addition to the sodium channel mutations previously reported,<sup>13–15</sup> we identified a germ line missense mutation in *GJA5* in a family with severe, early onset disease. This gene codes for the gap junction protein connexin40 (Cx40), which predominantly expresses in the atria and His-Purkinje system.<sup>16</sup> Heterologous expression experiments revealed that this novel mutation (Cx40-Q58L) significantly impaired the ability of Cx40 to form gap junction channels. Confocal microscopy showed that the Cx40-Q58L mutant but not the wild type (WT) failed to form plaques at sites of cell-cell apposition. Coexpression experiments indicated that the Cx40-WT protein provided only partial rescue of the Cx40-Q58L cellular phenotype. To our knowledge, this is the first description of a germ line mutation in a connexin gene associated with inherited ventricular arrhythmias. The results open the possibility of *GJA5* as a candidate gene for screening in patients with PFHBI, yet in the absence of further evidence, screening may be limited to the research environment rather than included as a part of the routine diagnostic examination.<sup>17</sup> The data also emphasize the importance of Cx40 in the maintenance of normal propagation in the specialized conduction system of the human heart.

## Methods

### Genetic Screening of PFHBI

Genomic screening by polymerase chain reaction and DNA sequencing was performed for *GJA5* (Cx40), *GJA1* (Cx43), *GJC1* (Cx45), *KCNQ1*, *KCNH2*, *SCN5A*, *KCNE1*, *KCNE2*, *KCNJ2*, *SCN1B*,

*SCN4B*, *HCN4*. Primer information is provided in the online-only Data Supplement. All participating probands and family members gave written informed consent in accordance with standards (Declaration of Helsinki) and local ethics committees.

### Plasmid Construction

A 1.1-kb Cx40-DNA fragment was subcloned into bicistronic plasmids pIRES2-EGFP and pIRES2-DsRED2. An EGFP or FLAG epitope was added at Cx40 C terminal to generate EGFP- or FLAG-tagged Cx40. Site-directed mutagenesis (Q58L) was performed with QuikChange. Primer information and additional details are provided in the online-only Data Supplement.

### Cell Culture and Transfection

Constructs were introduced into connexin-deficient HeLa cells or mouse neuroblastoma (N2A) cells using Lipofectamine as per manufacturer's protocol.

### Electrophysiology

Gap junction currents were recorded from transiently transfected N2A cell pairs using whole-cell double-patch clamp techniques as previously described.<sup>18,19</sup> Further details are provided in the online-only Data Supplement.

### Immunocytochemistry and Western Blotting

HeLa cells, transfected with pEGFPN1-Cx40-WT, pCMV-FLAG-Cx40-Q58L, or both, were stained with anti-FLAG M2 antibody and Alexa546-labeled secondary antibody. EGFP and Alexa546 fluorescence images were recorded by confocal microscopy. For western blotting, N2A cells were transiently transfected with 3  $\mu$ g of Cx40 plasmids. Two days after transfection, cells were lysed, and proteins were extracted and separated by conventional methods. Further details are provided in the online-only Data Supplement.

### Statistical Analysis

Results are presented as mean  $\pm$  SEM. Mann-Whitney rank sum tests with Bonferroni post hoc correction were used in comparisons for which normality or equal variance assumptions were invalid. In other instances, differences between groups were assessed by 1-way ANOVA followed by Bonferroni post hoc correction. Statistical significance was assumed for  $P < 0.05$ .

## Results

### Genetic Screening of PFHBI Probands

We genetically screened 156 probands given a clinical diagnosis of PFHBI. We identified 4 novel and 5 previously reported mutations in *SCN5A*,<sup>13,15</sup> 3 mutations in *SCN1B*,<sup>14</sup> and a novel germ line heterozygous missense mutation in exon 2 of the Cx40 gene *GJA5* (online-only Data Supplement Table I). Mutations were not found in connexin genes *GJA1* (Cx43) or *GJC1* (Cx45) or in the other genes screened (*KCNQ1*, *KCNH2*, *KCNE1*, *KCNE2*, *KCNJ2*, *HCN4*, or *SCN4B*). Of the novel *SCN5A* mutations, 1 caused a modification of the amplitude and voltage gating kinetics of the sodium current in heterologously expressing cells (online-only Data Supplement Figure I); 3 other mutant constructs failed to express functional channels, suggesting that patients carrying the mutation were functionally haploinsufficient for Nav1.5 (online-only Data Supplement Figure I). The *GJA5* mutation (c.173A>T) caused an amino acid substitution (glutamine [Q] replaced by leucine [L]) at position 58 in Cx40 (Cx40-Q58L) (Figure 1A and 1B). The mutation was absent in 400 alleles from unaffected control subjects and in the other 155 PFHBI probands. Screening of the entire gene

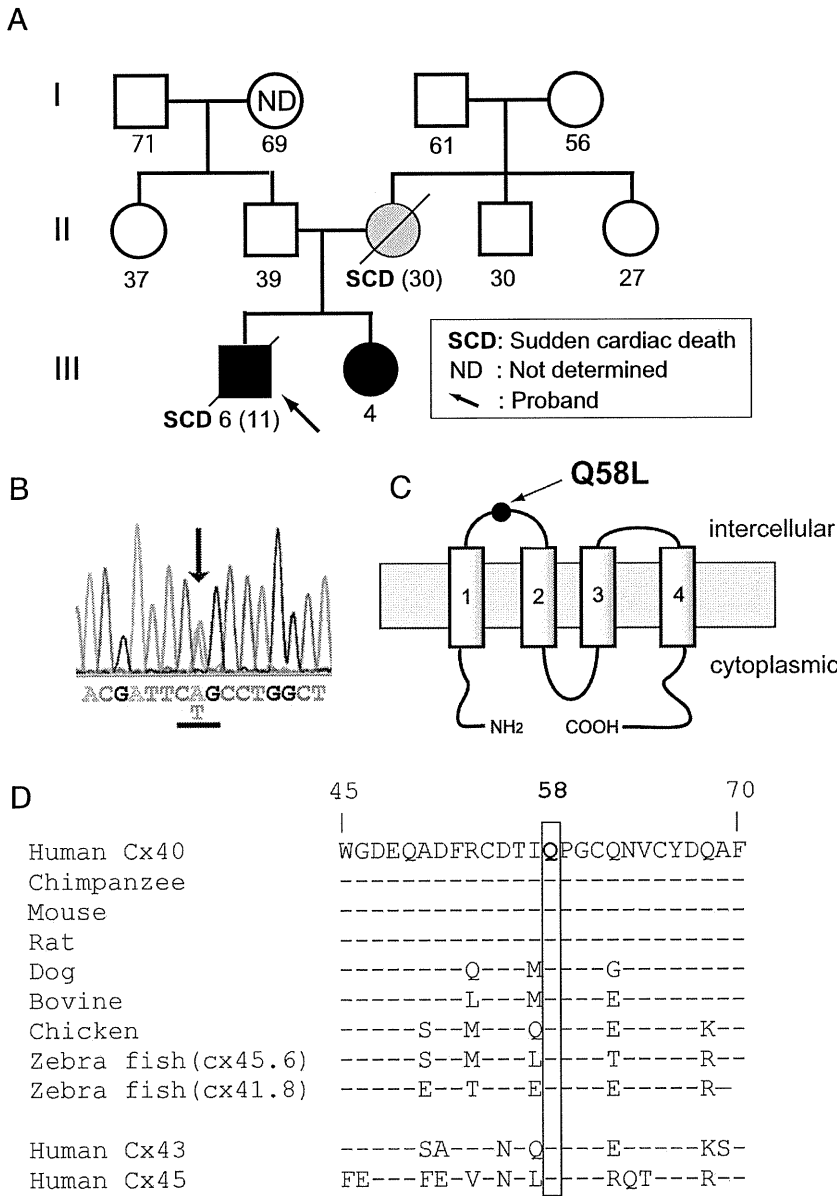


**Figure 1.** *GJA5* mutation identified in a family given the clinical diagnosis of progressive familial heart block type I. **A**, Family pedigree. Genetically affected and unaffected individuals are shown with closed and open symbols, respectively. The hatched circle indicates the proband's mother not genotyped; clinical data suggest that she was a de novo mutation carrier. Number below each symbol indicates the age at registration or age of SCD (parenthesis). **B**, Sequence electropherogram of exon 2 *GJA5* of proband. Arrow indicates heterozygous missense mutation of leucine (CTG) for glutamine-58 (CAG). **C**, Cx40 predicted membrane topology indicating position Q58 in first extracellular loop. **D**, Sequence alignment of human Cx40 and its homologues (residues 45–70). Notice the conservation in human Cx43 and Cx45. Dashes indicate residues identical with the top sequence. Cx indicates connexin.

panel (including *SCN5A* and *SCN1B*) revealed no other sequence modification in the DNA of this proband. Topological analysis placed amino acid 58 of Cx40 within the first extracellular loop (Figure 1C). The presence of glutamine in this position is highly conserved among *GJA5* orthologs, and 2 other cardiac connexins, Cx43 and Cx45 (Figure 1D). The clinical and genotypic characteristics of proband and tested family members are described next.

**Clinical Phenotypes and Genotype of the PFHBI Pedigree With the *GJA5* Mutation**

The proband, an 11-year-old boy at time of death, was first referred for evaluation when he was age 6 years because of ECG abnormalities. Although asymptomatic at that time, his ECG showed advanced atrioventricular block, complete left bundle branch block, and left axis deviation (Figure 2A). Echocardiography and cardiac scintigraphy did not reveal

signs of structural heart disease. He experienced an episode of syncope at age 9; implantation of a permanent pacemaker was recommended by the physician but not authorized by the legal guardian. The proband died suddenly 2 years later during exercise (running), and the family declined postmortem examination. The proband's younger sister shares the Cx40-Q58L mutation. She is asymptomatic, with a QRS duration at the upper limit of normal, left axis deviation that has been progressive (online-only Data Supplement Table II), and QRS notch. These findings are consistent with impaired intraventricular conduction (Figure 2B). The mother died suddenly at age 30 after delivering the second child. An ECG on record, obtained when she was age 16, was similar to that of the proband (compare Figure 2C with 2A). In addition, a ventricular tachycardia was recorded during the recovery phase of an exercise stress test (online-only Data Supplement Figure II). DNA from the mother was not available for



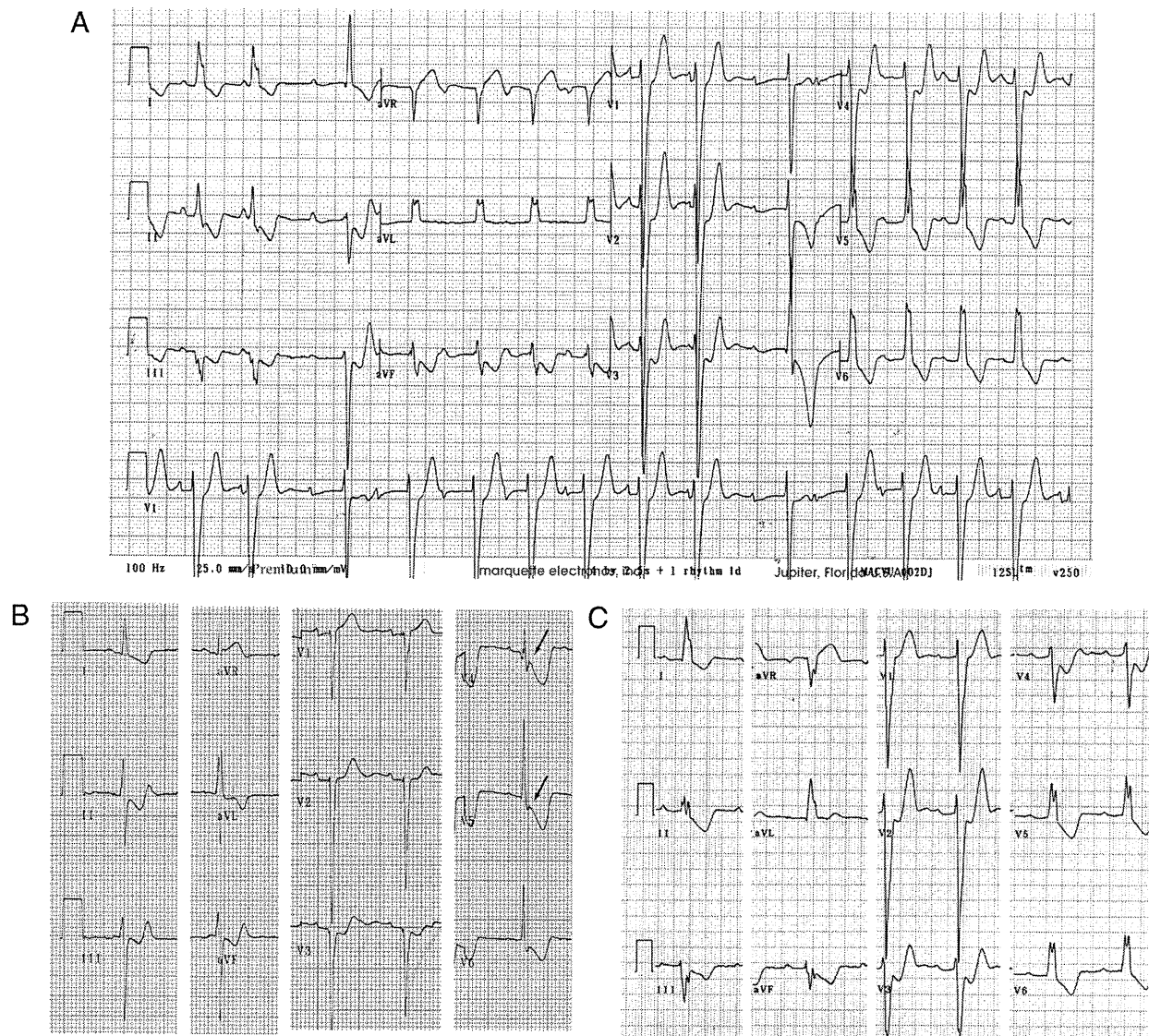


**Figure 2.** ECGs of proband and affected family members. **A**, ECG of proband at age 6 years, showing advanced atrioventricular block, complete left bundle branch block, and left axis deviation. Patient died suddenly 5 years later. **B**, ECG of proband's sister at age 6 years, showing QRS duration at the upper limit of normal, left axis deviation that has been progressive, and QRS notch in leads V4 and V5 (arrows) consistent with impaired intraventricular conduction. **C**, ECG of proband's mother at age 16 years, showing complete left bundle branch block and left axis deviation. She died suddenly at age 30.

examination. Other family members, including the proband's father, showed normal ECGs. DNA analysis of proband's father and maternal grandparents revealed absence of the Cx40-Q58L mutation. On the basis of clinical data and genotypic features of the proband and sister, it is most likely that the Cx40-Q58L mutation appeared *de novo* in the proband's mother. The data also indicate an early onset of PFHBI in this family compared with the natural history of the disease in most other cases.<sup>8</sup> As an initial step to assess the functional implications of the Cx40-Q58L mutation, modified constructs were transiently expressed in an exogenous system and evaluated for localization and function.

#### Electrophysiological Properties of Mutant Cx40-Q58L Channels

Connexin-deficient N2A cells were transiently transfected with cDNA for Cx40-WT or Cx40-Q58L; electrophysiological

properties of homologous Cx40 channels were analyzed by conventional dual whole-cell patch clamp. Figure 3A shows representative junctional current traces elicited by a transjunctional voltage gradient of  $-60$  mV. Average junctional conductance ( $G_j$ ) decreased from  $22.2 \pm 1.7$  nS in cells expressing Cx40-WT ( $n=14$ ) to  $0.56 \pm 0.34$  nS in cells expressing the Cx40-Q58L mutant ( $n=14$ ;  $P<0.001$ ). The probability of functional coupling, calculated by dividing the number of electrically coupled pairs by the number of pairs tested, was 100% and 57.1% for Cx40-WT and Cx40-Q58L, respectively.

Figure 3B depicts representative single-channel recordings elicited by a transjunctional voltage of  $-60$  mV in cell pairs expressing Cx40-WT or Cx40-Q58L. Unitary events for WT channels displayed current transitions corresponding to 2 conducting states ( $O_1$  and  $O_2$ ) of 43.3 and 119.5 pS, respectively. Figure 3C shows the event histograms for both cell

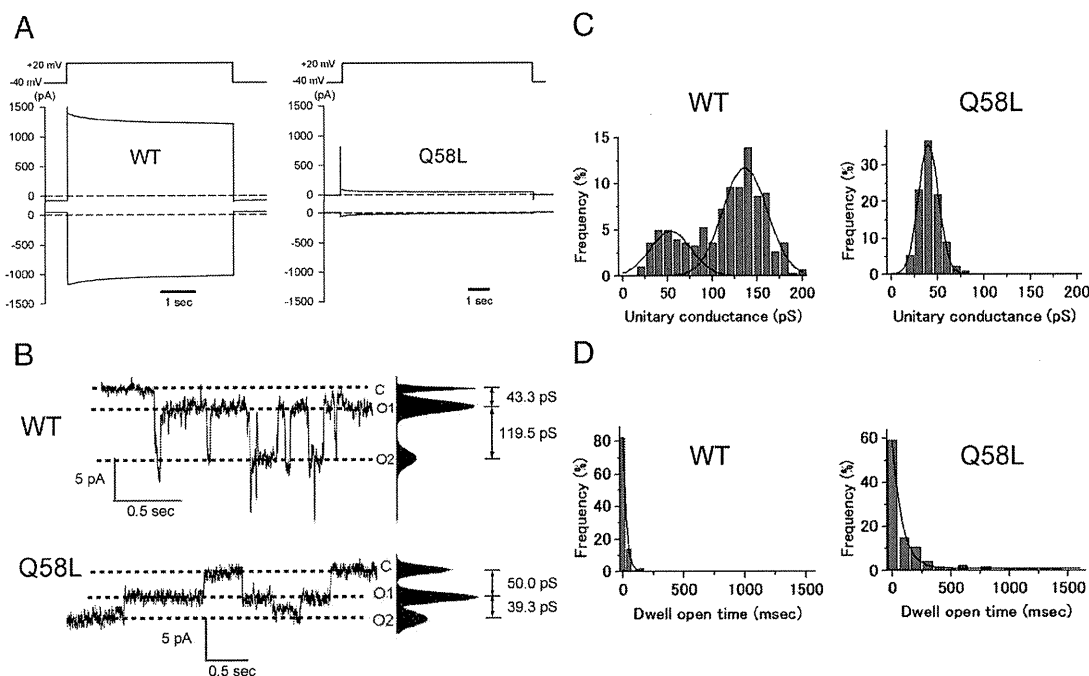


**Figure 3.** Whole-cell and single-channel properties of connexin40 (Cx40)-WT and Cx40-Q58L channels. **A**, Voltage pulse (top) and junctional current (bottom) from a homomeric WT cell pair (junctional conductance, 12.9 nS) and a Q58L cell pair (junctional conductance, 1.2 nS). **B**, Unitary currents recorded from homomeric Cx40-WT and Cx40-Q58L channels. O<sub>1</sub> and O<sub>2</sub> refer to 2 conducting (open) unitary levels of current. **C**, All-event histograms pooled from WT (n=3) and Q58L (n=3) cells with homologous channels. For WT, Gaussian peaks centered at  $136.2 \pm 2.3$  and  $53.1 \pm 5.3$  pS. For Q58L, best fit by a single Gaussian distribution centered at  $40.2 \pm 0.3$  pS (n=3). **D**, Frequency of events in relation to dwell open time. Binned data were fit by single exponentials ( $\tau_{\text{open}}$  WT,  $27.9 \pm 0.5$  ms, 4 cells, 186 events;  $\tau_{\text{open}}$  Q58L,  $92.0 \pm 7.8$  ms, 3 cells, 163 events). WT indicates wild type.

types (Cx40-WT, 3 cell pairs and 303 events; Cx40-Q58L, 3 cell pairs and 416 events). The histogram for the Cx40-WT channels was best described by 2 Gaussian distributions centered at  $136.2 \pm 2.3$  and  $53.1 \pm 5.3$  pS. In contrast, the histogram for Cx40-Q58L channels was best described by a single Gaussian function centered at  $40.2 \pm 0.3$  pS. Moreover, the length of time that a channel dwelled in the open state (dwell open time) was substantially longer for the Cx40-Q58L channels ( $92.0 \pm 7.8$  ms, 3 cell pairs, 163 events) than for Cx40-WT channels ( $27.9 \pm 0.5$  ms, 4 cell pairs, and 186 events) (Figure 3D). Of note, the Q58L mutation had a strong dominant effect on formation of heterotypic functional gap junctions. Cells were transfected with either pIRES2-EGFP-Cx40-WT or pIRES2-DsRED2-Cx40-Q58L, and heterotypic pairs were identified by fluorescence microscopy (an EGFP-expressing cell paired with a DsRED2-expressing cell). We recorded from 8 cell pairs and detected unitary current events in only 2 pairs. A total of 57 events were recorded, and average macroscopic junctional conductance was  $0.04 \pm 0.03$  nS. Collectively, the data demonstrated that the Q58L mutation significantly affects the biophysical properties of Cx40 channels and the overall ability of Cx40 gap junctions to form a low-resistance pathway between cells.

### Electrophysiological Properties and Gap Junction Plaque Formation in Cells Coexpressing WT and Q58L Proteins

In the clinical cases identified, the Q58L mutation was detected in only 1 carrier allele. Therefore, we assessed the

function of gap junctions in cells coexpressing WT and mutant proteins. N2A cells were cotransfected with cDNA for both GFP-tagged Cx40-WT and Cx40-Q58L ( $0.5 \mu\text{g}$  of pEGFPN1-Cx40-WT combined with  $0.5 \mu\text{g}$  of pEGFPN1-Cx40-Q58L). Results were compared with those obtained when only 1 of the constructs ( $1 \mu\text{g}$ ) was transfected. Cells expressing both constructs (WT/Q58L) showed intermediate conductance ( $15.4 \pm 3.7$  nS, n=16) between WT ( $28.8 \pm 3.6$  nS, n=16,  $P < 0.001$ ) and Q58L ( $0.28 \pm 0.11$  nS, n=14,  $P < 0.001$ ) (Figure 4A). These values were comparable to those obtained using the bicistronic pIRES2-EGFP constructs (WT,  $22.2 \pm 1.7$  nS, n=14; WT/Q58L,  $13.0 \pm 2.4$  nS, n=17; Q58L,  $0.56 \pm 0.34$  nS, n=14). The coexpression results were consistent with those obtained using pIRES plasmids that tagged the cells both green and red, if cotransfected (online-only Data Supplement Figure I). The probability of finding functional coupling in cotransfected cells was 76.5%, which was intermediately between WT (100%) and Q58L (57.1%).

The characteristics of gap junction plaques observed in cells coexpressing WT and Q58L varied significantly between pairs (Figure 4B). Nearly one half of transfected (fluorescence-positive) cells exhibited clear and discrete gap junction plaques (arrow a), whereas the rest of fluorescence-positive cells showed a diffuse expression pattern and absence of well-defined plaques (arrow b). Fluorescence-positive and gap junction plaque-positive cells were counted in 10 different views for each group, and efficacy of gap junction plaque formation was statistically analyzed (Figure 4C) by calculating the ratio of cells with gap junction plaques

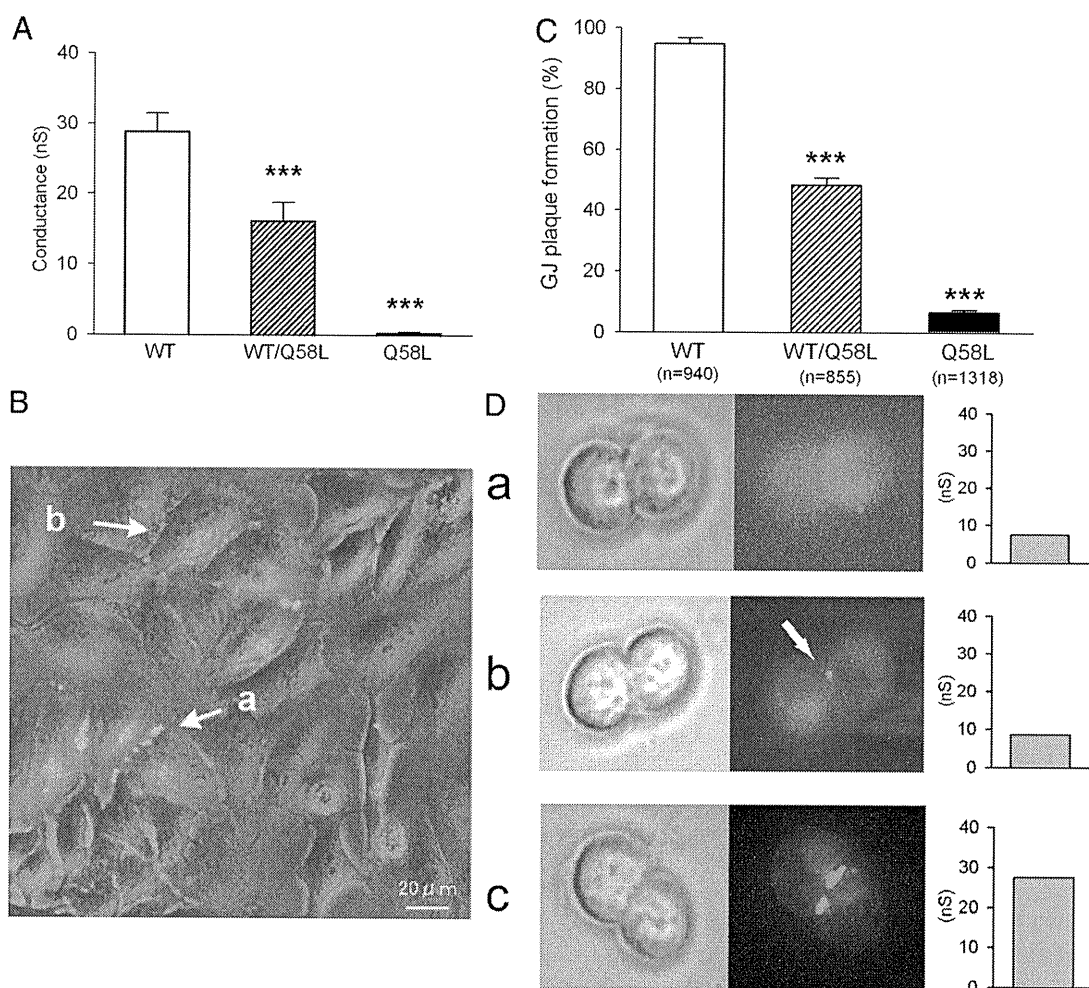


**Figure 4.** Macroscopic conductance and gap junction plaque morphology in cells coexpressing connexin40 (Cx40)-WT and Cx40-Q58L. **A**, Junctional conductance of cells transfected with plasmid pEGFPN1-Cx40-WT (1  $\mu$ g), pEGFPN1-Cx40-Q58L (1  $\mu$ g), or cotransfected with WT and Q58L (WT/Q58L, pEGFPN1-Cx40-WT 0.5  $\mu$ g+pEGFPN1-Cx40-Q58L 0.5  $\mu$ g). **B**, Phase contrast/fluorescence overlay image of neuroblastoma cells transfected with WT/Q58L constructs. Arrow *a* points to gap junction plaque; arrow *b* points to an example of cells transfected but devoid of gap junction plaque. **C**, Efficacy of gap junction plaque formation was measured as the ratio between the number of gap junction plaque-positive cells and the number of fluorescence-positive cells (WT, n=940; WT/Q58L, n=855; Q58L, n=1318). **D**, Representative images of phase contrast (left), EGFP fluorescence (middle), and junctional conductance (right) from neuroblastoma cells cotransfected with pEGFPN1-Cx40-WT (0.25  $\mu$ g) and pEGFPN1-Cx40-Q58L (0.25  $\mu$ g). Three different examples illustrate the relation between plaque morphology and recorded junctional conductance. WT indicates wild type. \*\*\* $P$ <0.001 compared with WT.

to the number of fluorescence-positive cells. In the Cx40-WT group, almost all fluorescence-positive cells exhibited clear gap junction plaques ( $94.9 \pm 1.9\%$ , n=940), whereas there was a more-diffuse and homogenous pattern with only occasional plaque formation in the Cx40-Q58L group ( $6.6 \pm 0.7\%$ , n=1318,  $P$ <0.001 compared with WT). In contrast, results varied widely in cells cotransfected with WT/Q58L; nearly one half of fluorescence-positive cells exhibited gap junction plaques similar to those observed in cells transfected with the WT construct ( $48.2 \pm 2.4\%$ , n=855,  $P$ <0.001), whereas the rest showed a diffuse expression pattern similar to that of Cx40-Q58L. To establish a better correlation between plaque formation and junctional conductance, both variables were measured concurrently in the same cell pair for 39 N2A cell pairs where GFP-tagged plasmids of Cx40-WT and Cx40-Q58L were cotransfected. As shown in Figure 4D, about one half of GFP-positive cell pairs showed

a very small G<sub>j</sub> (<5 nS) and very few or negligible gap junction plaques (a). In the other half of cell pairs, small, dot-like junctional plaques correlated with intermediate G<sub>j</sub> values (b), and there were clear, extensive gap junction plaques associated with G<sub>j</sub> values >25 nS (c). Overall, we found significant heterogeneity in the extent of electric coupling, although the measurements of G<sub>j</sub> correlated with the localization of proteins in transfected cells. These results indicate that the Q58L mutation significantly impairs the ability of cells to form gap junction plaques, although the effect is not purely dominant when both WT and mutant proteins are coexpressed.

#### Subcellular Distribution of WT and Q58L Cx40 in Transiently Transfected Cells

To further analyze the subcellular distribution of Cx40-WT and Cx40-Q58L proteins, the C terminal of Cx40-WT was

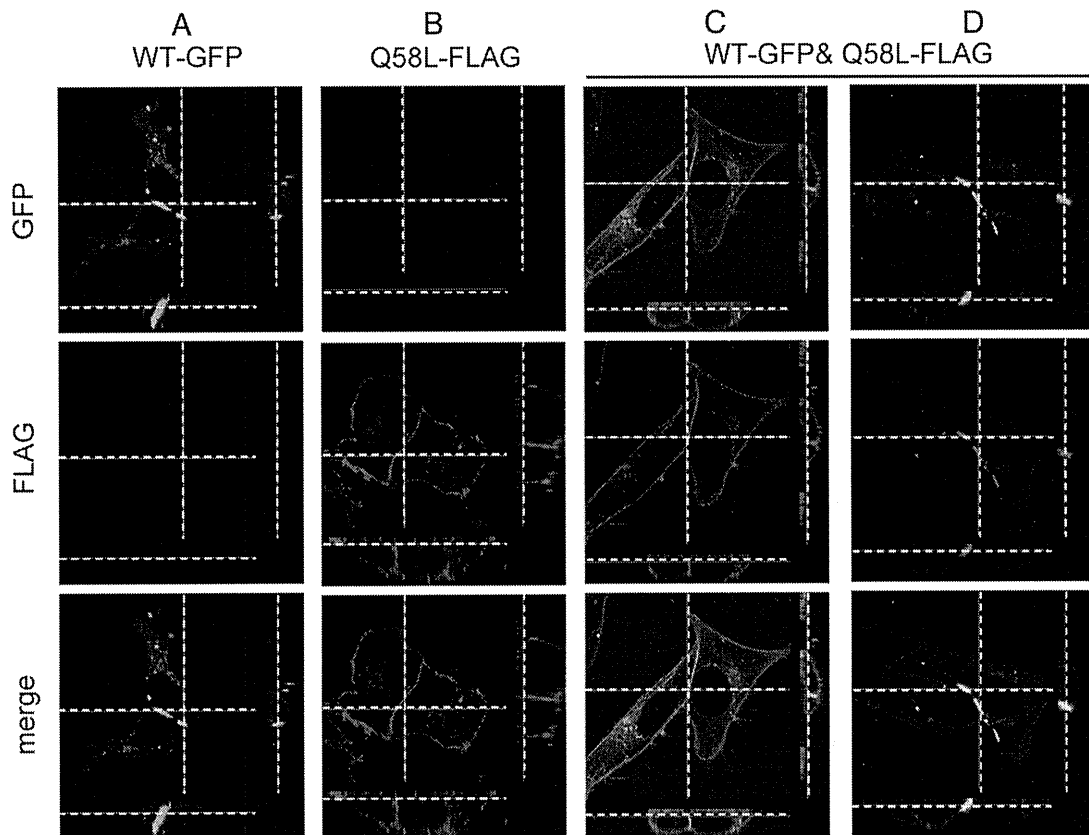


**Figure 5.** Subcellular distribution of connexin40 (Cx40)-WT and Cx40-Q58L in transiently transfected cells. HeLa cells were transiently transfected with pEGFPN1-Cx40-WT (3.0  $\mu$ g) (A), pCMV-FLAG-Cx40-Q58L (3.0  $\mu$ g) (B), or pEGFPN1-Cx40-WT (1.5  $\mu$ g) plus pCMV-FLAG-Cx40-Q58L (1.5  $\mu$ g) (C); immunostained for the respective tag protein; and visualized by confocal laser scanning microscopy. Notice that gap junction plaques (A) are absent in Q58L transfectants (B) and present in some (D) but not all (C) cotransfected cells. Bar=20  $\mu$ m. WT indicates wild type.

tagged with GFP, whereas the C terminal of Cx40-Q58L was FLAG tagged. After transfection of N2A cells with the tagged constructs, the distribution of each protein was examined by confocal microscopy. As shown in Figure 5, green color indicates the position of GFP-tagged molecules, whereas red indicates the position of FLAG-tagged molecules. In cells transfected only with GFP-tagged Cx40-WT, fluorescence was consistently detected at sites of cell-cell apposition, following the pattern previously described for GFP-labeled gap junction plaques (Figure 5A). A similar distribution was found when cells were transfected with FLAG-tagged Cx40-WT (not shown). In contrast, most FLAG-tagged Cx40-Q58L signals were evenly distributed around the cell in the vicinity of the plasma membrane (Figure 5B). Biotinylation experiments showed that the Q58L mutation did not prevent the Cx40 protein from inserting into the membrane and presenting a domain-reachable form in the extracellular space (online-only Data Supplement Figure II). Microscopy experiments in cells coexpressing GFP-tagged Cx40-WT and FLAG-tagged Cx40-Q58L proteins yielded results intermediate to those obtained when only 1 construct was expressed. Nearly one half of cell pairs showed that both proteins distributed homogeneously at or near the cell membrane, without the formation of well-defined gap junction plaques (Figure 5C). These images resembled those obtained when

only Cx40-Q58L proteins were expressed (Figure 5B, FLAG). In contrast, other cell pairs showed clustering of fluorescent signals within closely confined areas that appeared to be gap junction plaques (Figure 5D).

The experiments described herein led us to speculate that the distribution and function of heteromeric connexons is determined by their mutant subunit content, whereby formation (or not) of plaques and channels are determined, at least in part, by the abundance of expression of one protein over the other. As an initial step to probe this hypothesis, we took advantage of the characteristics of the bicistronic plasmid pIRES, in which the expression rate of the upstream gene is several-fold greater than that of the downstream gene,<sup>20</sup> and explored the functional properties of heteromeric connexons. Cx40-WT and GFP-tagged Cx40-Q58L were subcloned into the pIRES vector, either alone or in combination, in the specific orientations shown in Figure 6A. Protein expression levels of Cx40-WT and Cx40-Q58L were determined by immunocytochemistry. In contrast to the data obtained when Cx40-WT and GFP-tagged Cx40-Q58L plasmids were cotransfected at a 1:1 ratio (lane 6), expression of heteromeric pIRES plasmids WT-IRES-Q58L-EGFP (lane 3) and Q58L-EGFP-IRES-WT (lane 4) resulted in uneven protein expression levels of WT (40 kDa) and Q58L-EGFP (67 kDa), depending on their orientation in the pIRES vector. Based on